ANALYSIS OF CURRENT FLOW PATH AND TEMPERATURE DISTRIBUTION OF Ag-NANOWIRE NETWORK USING THERMOREFLECTANCE IMAGING

Y. SUGIHARA[1], R. UEMURA[1], K. TAMAI[1], R. Kuriyama[1,2] and K. TATSUMI[1]

1. Department of Mechanical Engineering and Science, Kyoto University
Kyotodaigakukatsu, Nishikyo-ku, Kyoto 615-8540, Japan

2. Japan Science and Technology Agency, PRESTO Researcher

* Corresponding Author: e-mail address (tatsumi@me.kyoto-u.ac.jp)

Keywords: Ag nano-wire, Network, Contact resistance, Joule heating, Thermo-reflectance Imaging

ABSTRACT

A sheet consisted of Ag nano-wire (Ag-NW) which is randomly dispersed and forming a network can be applied to electronic devices and wearable devices as flexible and transparent conductive film material and heater. To evaluate the performance and reliability of the sheet and device, it is necessary to investigate and understand the characteristics of the current and temperature distribution of the Ag-NW network. The current path is based on the dispersed pattern of the Ag-NWs and the electric and thermal resistances of the Ag-NWs and contact point of the Ag-NW junction. These resistances change depending on the properties of the polymer coating of the Ag-NW and contact conditions at the junction. Therefore, it is important to analyze the characteristics of the current and temperature distributions in the Ag-NW network, and evaluate the degree of the contact resistance variation and their effect on the current and temperature distribution. In this study, we measured the temperature distribution of Joule-heated Ag-NW network using thermoreflectance imaging (TRI). Numerical computation was conducted for the electric current flow and heat transfer of the Ag-NW network. The contact electric resistance was obtained by solving the optimization problem to minimize the difference between the temperature distributions of the measurement and computation. The results showed that the contact electric resistance varies over the Ag-NW network at certain magnitude. This variation significantly affected the temperature distribution by defining the current path and producing a non-uniform current distribution.

INTRODUCTION

A sheet consisted of Ag nano-wires (Ag-NWs) gives high electric conductivity, and furthermore, it can become flexible and transparent if the layer thickness and concentration of the NWs are small(1). The sheet can also be used as flexible film heater(2). Therefore, Ag-NW sheet is considered to be a promising material which can be applied to electronic devices and wearable devices.

High conductivity and heating performance can be obtained when the current flows uniformly over the NWs. However, limitation of the paths of the current are observed in the actual NW network and the current shows non-uniform distribution. This is attributed to the connecting pattern of NWs and the variation of the resistance at NWs and contact points. The non-uniform current distribution affects the Joule heating and generates high temperature regions (hot-spots) which can lead to thermal fatigue of the NW network. Therefore, it is important to understand the characteristics of the current path and temperature distribution of the NW network, and evaluate the effect of the contact resistance variation on these distributions to provide insight into the design of high performance and reliable NW network.

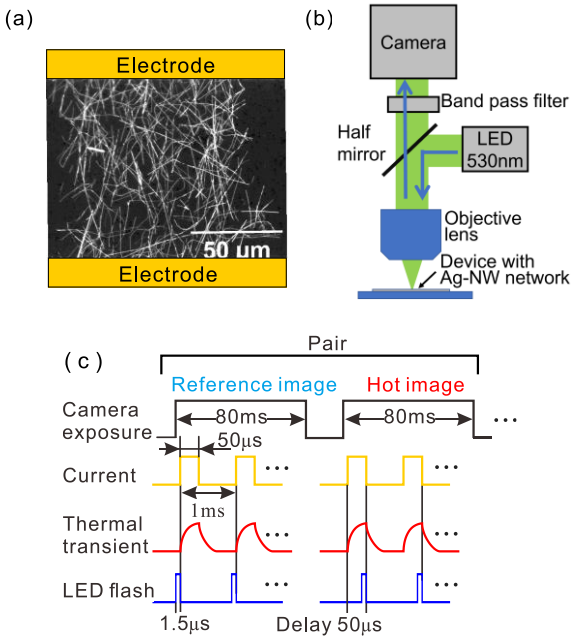

Figure 1. (a) Photograph of the Ag-NW network dispersed on glass substrate between Au electrodes, and (c) optical system and (b) timing chart of the TRI measurement.

The contact electric resistance changes depending on the properties and thickness of the polymer coating of the Ag-NW which is generally applied to the Ag-NWs to keep the properties and strength of the Ag-NW stable. The contact condition of the Ag-NWs can affect the resistance also. However, although contact electric resistance at a single point of two Ag-NWs have been investigated(3), the variation of the resistance in the Ag-NW network has not be elucidated. Further, the current distribution - current path – in the Ag-NW network has not been measured. This is due to the difficulty in the measurement of the current in two-dimensional form and sub-micrometer scale, which is difficult in the temperature measurement as well.

In this study, we measured the two-dimensional temperature distribution of the current-applied-Ag-NW network using the thermo-reflectance imaging (TRI) technique. TRI can measure the two-dimensional temperature of the material surface with the accuracy of sub-micrometer in space, and sub-microsecond in time.

We further conducted numerical computation for the electric current and heat transfer of the NWs and estimated the contact electric resistance (contact electric conductance) at the NW junction by matching the temperature distribution of the Ag-NW network to the measurement. Discussion is made on the path and non-uniformity of the current and its resulting temperature distribution. We evaluated the degree of the contact electric resistance variation by comparing the current and temperature distributions with the case of uniform contact electric resistance, and how the contact electric resistance contributes to the generation of the current path and temperature distribution.

METHODS

Measurement sample

Fig. 1 (a) shows the photograph of the Ag-NW-network. Ag-NWs with diameter of 120-150 nm and length of 20-50 μm (Sigma-Aldrich: #739448) were dispersed on the glass substrate in the area located between two parallel Au electrodes using vacuum filtration method. Au parallel electrodes were patterned on the glass substrate using the lithography and electron beam vapor deposition methods. The distance between the electrode was 100 μm. In the vacuum filtration, a thin layer of Ag-NWs was deposit on the porous filter. Ag-NWs located outside the area of the deigned pattern were first removed, and the remaining Ag-NWs were transferred to the glass substrate at the area between the electrodes. The width of the area where the Ag-NWs was transferred was 100 μm, therefore the measured area was square 100 μm on a side. The concentration of the Ag-NWs represented by the total length of the Ag-NWs per unit area was 8.3×10^5 m^{-1}. The electric resistance of Ag-NW network (the area between the electrodes) was 18.7 Ω.

Thermo-reflectance imaging

The TRI measures the two-dimensional distribution of the surface temperature utilizing the phenomenon that the reflectance of the material changes with temperature (thermo-reflectance). The surface temperature can be obtained by measuring the reflectance and applying it to the following relationship.

$$\Delta R = \frac{\partial R}{\partial T}\Delta T \tag{1}$$

R and T are the reflectance and temperature, respectively. Having the intensity of the reflected light given as I, we get the relationship between the variation of I and T as follows.

$$\frac{\Delta I}{I} = \left(\frac{1}{R}\frac{\partial R}{\partial T}\right)\Delta T = C_{\mathrm{TR}}\Delta T \tag{2}$$

In Eq. (2), the part enclosed in parentheses is called thermo-reflectance coefficient C_{TR}. The value of C_{TR} is a physical property of the material and depends on the wavelength of the light.

Table 1. Properties and parameters of the computation

Parameter	*Values*
Contact thermal conductance (W/K)	1.0×10^{-7}
Ag-NW	
Diameter (nm)	135
Density (kg/m^3)	1.05×10^4
Specific heat capacity (J/(K·kg))	234
Electric resistivity (Ω·m)	1.58×10^{-8}
Thermal conductivity (W/(m·K))	420
Glass substrate	
Density (kg/m^3)	2.5×10^3
Specific heat capacity (J/(K·kg))	670
Thermal conductivity (W/(m·K))	0.65

Fig. 1 (b) shows the schematic of the optical system of the measurement. LED light was used as the incident light in the measurement. The light was irradiated to the object through a half mirror and objective lens (Olympus, LMPLFLN 100X NA=0.8). The reflection image was recorded using a CMOS camera (Hamamatsu Photonics, ORCA Fusion). The pixel resolution of the system was 65nm/pixel. Autofocus system was installed in the measurement system to keep obtaining the focused images during the measurement. Autofocus operated by irradiating light of bandwidth of 530 nm to the object and measuring the periodic pattern generated at the surface. Therefore, bandpass filter was inserted before the camera to cut the light of the autofocus system and measure the reflected light of the LED only.

Current was periodically applied to the electrode in a form of square pulse with width of 10 μs and period of 250 μs. Reflectance was measure by LED flash light with width of 1.5 μs and period of 250 μs. The nominal wavelength of the LED light was 530 nm. Timing of irradiation was adjusted to the phases at which the Ag-NW gives the maximum temperature and the temperature equal to room temperature, respectively. The former image was referred to as hot-image, and the latter as reference-image. The timing chart of the measurement is shown in Fig. 1 (c).

Five thousand pairs of the images were measured. The temperature difference ΔT of each pair was calculated and ΔT was averaged over 5,000 pairs. The reflectance was converted to temperature using the TR coefficient C_{TR} of 8.96×10^{-5} K^{-1}. This value was obtained from the calibration measurement on C_{TR} for Ag conducted by the authors using the TRI system and Ag plane mirror.

Computation

Numerical computation was conducted to solve the current and temperature distribution of the Ag-NW network. The conservation equations of electric current and energy (heat transfer) of the NWs was solved in the computation. The voltage applied to the electrode and the total current supplied to the Ag-NW were adjusted to those of the measurement. The contact electric resistance of the NWs was derived to make the temperature distribution of the computation fit with that of the measurement by solving the minimization problem of the loss function for the

temperature difference at each divided segment of the NWs. In the computation, we used the contact electric conductance which is the inverse value of resistance. Therefore, it should be noted that hereafter contact electric conductance will be used to explain the numerical procedure and presented in some of the results and discussion.

The heat transfer computation considered the heat conduction of the NWs, heat transfer at the contact point of the NW junction, and heat transfer to the glass substrate. The temperature of the glass substrate was kept constant as the heating time was 10 μs for the hot-image, and temperature change of the substrate during this time was negligible. Thermal conductivity at the contact point of the NW junction, and the physical properties of the Ag-NW and glass were referred to other works. The properties and values of the parameters are summarized in Table 1.

Numerical procedure

Contact electric conductance k of the NW junction and the contact thermal conductance between the NW and glass substrate were calculated by the following procedure.

The value k was calculated by minimizing the loss function L defined as Eq. (3) representing the temperature in vector format.

$$L = |\alpha \boldsymbol{T}_\mathrm{s} - \boldsymbol{T}_\mathrm{m}|^2 \tag{3}$$

$\boldsymbol{T}_\mathrm{s}$ is the calculated temperature, $\boldsymbol{T}_\mathrm{m}$ is the measured temperature, and α is the correction coefficient. α was applied to correct the difference in the overall temperature between the measurement and computation. This difference appeared due to having the contact thermal conductance between the NWs and glass substrate α_g initially unknown. The contact electric conductance and contact thermal conductance contributes to the current and temperature distribution of the NW network. On the other hand, the contact thermal conductance between the NWs and glass substrate mainly affects the overall temperature as the temperature of the glass substrate is constant during the heating of the Ag-NWs. The α was calculated as Eq. (4) using the temperature $\boldsymbol{T}_\mathrm{s}$ at each moment.

$$\alpha = (\boldsymbol{T}_\mathrm{s} \cdot \boldsymbol{T}_\mathrm{m})/\boldsymbol{T}_\mathrm{s}^2 \tag{4}$$

Once α was applied, the value k of each NW junction which minimize L was calculated. The number of iteration to calculate k was 3,000, and the variation of L was 3.4×10^{-4} % in the last 300 steps. To match the overall electric resistance of the area to the measurement, we corrected the value of k by multiplying k of all junctions with constant magnitude.

Every 100 iteration steps of the calculation for k, α_g was updated finding the value which minimize the loss function shown in Eq. (5) using the dichotomous exploration method.

$$L = |\boldsymbol{T}_\mathrm{s} - \boldsymbol{T}_\mathrm{m}|^2 \tag{5}$$

RESULTS AND DISCUSSION

Temperature distribution

Fig. 2 shows the temperature of the Ag-NWs obtained by the measurement and computation. The pattern of the Ag-NWs is the same with the one shown in Fig. 1(a). Fig. 2 (a) shows the temperature of the TRI measurement. Non-uniform distribution of temperature and hot-spots generation are found showing that the current does not flow uniformly in the network and specific paths are formed. Several NWs join at some of the junctions, and the current paths converge to the junction. This produces high concentration current and large Joule heating leading to the generation of hot-spots.

Fig. 2 (b) shows the temperature distribution obtained by the computation calculating k of the junctions to make the temperature match with the measurement. Comparing Fig. 2 (a) and (b), the results of the computation agree well with the

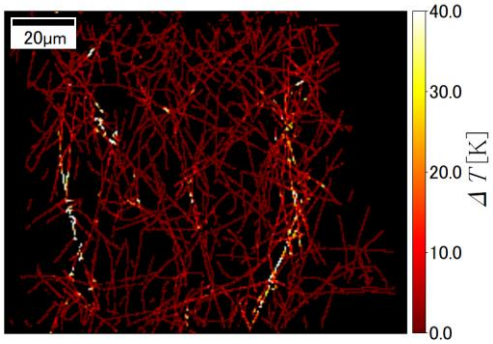

(a) TRI measurement

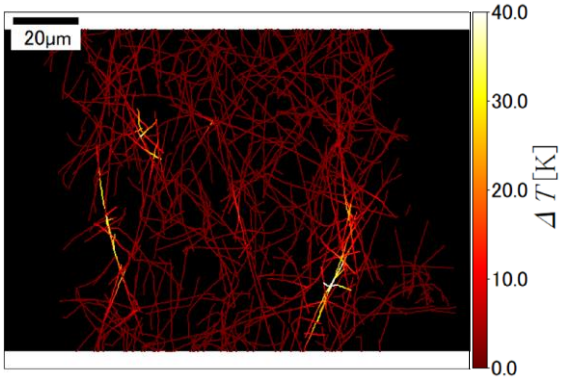

(b) Computation (adjusted contact conductance)

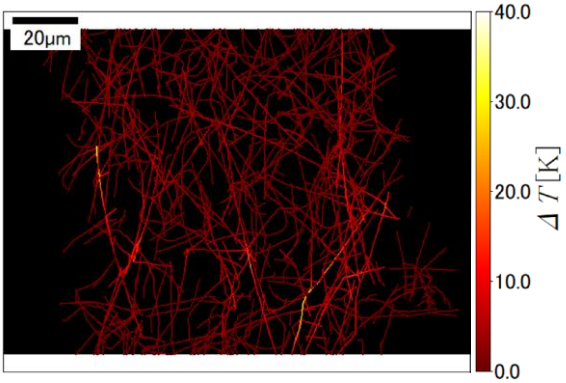

(c) Computation (uniform contact conductance)

Figure 2. Distribution of the temperature increase ΔT of the Ag-NW network obtained by TRI measurement and computation. The results of the computation show the cases of contact electric conductance adjusted at each junction, and applying equal value to all junction (uniform value).

measurement. The minimum value of the contact electric resistance was 95.3 Ω. The resistance varied in the range of approximately 100~50 × 10^4 Ω.

Fig. 2 (c) shows the result of the computation in which the value of k was kept equal for all Ag-NW junctions. The value was defined so as the overall resistance matched the measurement. Comparing the results with Fig. 2 (b), the temperature of the high temperature region, especially the hot-spots, decreases and a more uniform distribution is obtained. Further, we identified the junctions which significantly contributed to the temperature pattern by evaluating the sensitivity of the temperature distribution to the value k of each junction. The number of these key junctions was 178 out of total number of junctions 2358. The evaluation method used here will be mentioned in the next section.

These results show that the variation of k increases the non-uniformity of the temperature distribution, and the value of k of a limited number of junctions dominated the current and temperature distributions in the case k varies.

The junction with large k obstructed the current flow and limited the path in the Ag-NW network. This produced high current density regions and was the cause of the hot-spot generation. This concludes that, it is important to evaluate not only the dispersion pattern of the NWs but the variation of the contact resistance to understand the temperature distribution of the Ag-NW network.

Electric resistance and its effects

To evaluate the accuracy of the estimated contact electric resistance of the analysis, we numerically created an Ag-NW network consisted of randomly placed Ag-NWs. The contact electric conductance was applied randomly to the junction. The current, Joule heating, and temperature distributions were calculated by computation. We further applied Gaussian noise with standard deviation of 5K to the temperature of each segment. Using this data as a reference temperature distribution, we conducted the computation which was used in the previous section to calculate the contact electric conductance of the reference network. The results giving the estimated values were compared with those of the reference data initially applied. The temperature distribution of the reference data and that obtained by the computation are shown in Fig. 3. The two values agree well indicating the validity of the computation.

The accuracy of the estimated contact electric resistance was evaluated based on an error parameter r shown in Eq. (6)

$$r = \frac{|k_\mathrm{e} - k_\mathrm{t}|}{k_\mathrm{t}} \tag{6}$$

k_e and k_t are the estimated value and the applied one (the reference data) of the contact electric conductance, respectively. Fig. 4 (a) shows the frequency distribution of r. Although the temperature distribution agrees with the reference data, r is large and the accuracy is low for many junctions. As k is estimated from the temperature distribution, k cannot be defined specifically for the junctions located in the area where the temperature variation is small due to the lack of information. These areas correspond to the Ag-NWs with zero or negligibly small currents, and the contribution

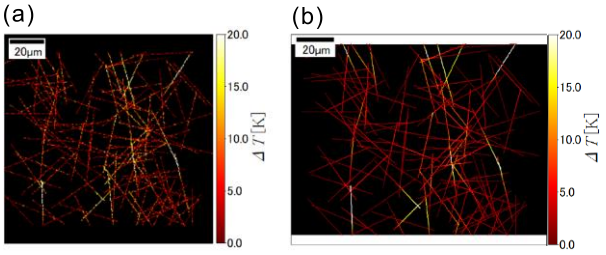

Figure 3. Distribution of the temperature increase ΔT of the Ag-NW network in the case of (a) reference data, and (b) obtained by the computation estimating the contact electric conductivity by matching the temperature to the reference data (a).

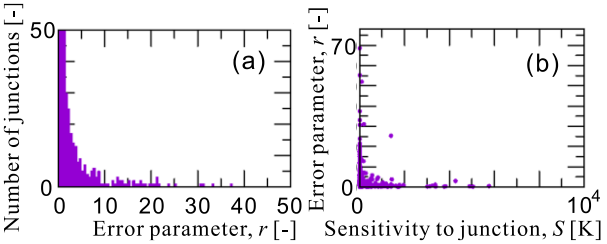

Figure 4. (a) Frequency distribution of error parameter r for the NW junctions, and (b) relationship between the r and sensitivity of the temperature distribution to the contact electric conductance of a junction.

of these junctions on the current path and temperature distribution is believed to be small.

We defined another evaluation function as shown in Eq. (7) which gives the sensitivity of the network temperature distribution to the variation of k of a junction.

$$S_\mathrm{i} = |\boldsymbol{T}_\mathrm{H} - \boldsymbol{T}_\mathrm{L}| \tag{7}$$

$\boldsymbol{T}_\mathrm{H}$ and $\boldsymbol{T}_\mathrm{L}$ are the vectors representing the network temperature when k of junction i was change to 10 Ω^{-1} and 10^{-10} Ω^{-1}, respectively. The relationship between S and r of all junctions were examined for several reference networks. The results are shown in Fig. 4 (b).

In Fig. 4 (b), junction with large S gives small r showing an inverse correlation. Further, the number of junctions with large S is small. This indicates that only a limited number of junctions contributes to the formation of the current path and temperature distribution.

This procedure was used to the evaluate the contribution of the contact electric resistance of the junction to the temperature distribution obtained by the measurement. As previously mentioned, the number of junctions of $S > 5.0\times10^3$ was 178 out of 2358 which is the number of all junctions. This shows that if the electric resistance of such key junction changes to some extent, the pattern of the current path and the current density of the NWs can easily change. This will lead to the change of the temperature distribution and number of hot-spots.

Figs. 5 and 6 respectively show the current distribution and the electric conductivity k at the junctions obtained by the simulation matching the temperature distribution of the measurement, namely the current distribution which gives ΔT shown in Fig. 2 (b). In Fig. 6 the values of k only at the

junctions of which the sensitivity parameter S is greater than 1,000 K^2 are plotted.

The distribution shown in Fig. 5 is non-uniform and shows several paths with current of large values. The location of large current corresponds to that of large ΔT shown in Fig. 2 (b). This is reasonable as the temperature increase is caused by Joule heating. On the other hand, the magnitude of ΔT at the hot-spot is more conspicuous and the distribution gives greater contrast compared to the current distribution. The reason for this is twofold. One is that Joule heating is proportional to the square of current. Therefore, the variation in the distribution increases in the case of ΔT. The other reason is the effect of heat transfer. Although the heating time (current applied time) is 10 μs, heat transfer occurs during this period in the Ag-NW network. In the area of small current, the number of connected Ag-NWs is large and the apparent electric conductivity of the area is large. This Ag-NW structure affects the heat transfer in a similar way, that the apparent heat conduction and thermal diffusivity is large in the area resulting in decrease of ΔT at points of small ΔT.

In Fig. 6, the junctions of large S is concentration along the current path, and the value of k shows both large and small values. The junctions of small k obstruct the current flow and the junctions of larger k is the point at which the current flows and concentrates. The combination of these two generates the current path shown in Fig. 5. These results represents that the contact electric resistance variation should be considered carefully to evaluate the current path and temperature distribution of the Ag-NWs network.

CONCLUSION

Temperature distribution of the current-supplied Ag-NW network was measured using thermo-reflectance imaging. The current distribution and the contact electric resistance of the Ag-NW network was obtained numerically by matching the temperature distribution with the measurement. The contact electric resistance varied at each junction, and played an important role in generating specific current paths and hot-spots in the Ag-NW network. The results showed that the performance and reliability of conductive sheets and heaters using Ag-NW network should consider the effect of the variation and reliability of the contact electric resistance, which similarly could occur with the contact thermal resistance.

NOMENCLATURE

C_{TR}:	thermo-reflectance coefficient	[K]
I:	light intensity	[-]
k:	contact electric conductance	[1/Ω]
L:	loss function	[K^2]
R:	reflectance	[-]
T:	temperature	[K]
α:	correction coefficient	[-]
α_g:	contact thermal conductance	[W/K]

Subscripts

s: computation
m: measurement

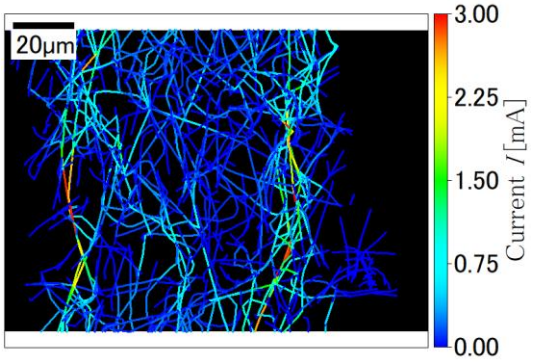

Figure 5. Current distribution of the Ag-NW network obtained by the computation in the case of matching the temperature to the measurement: the distribution corresponds to the results of ΔT shown in Fig. 2 (b).

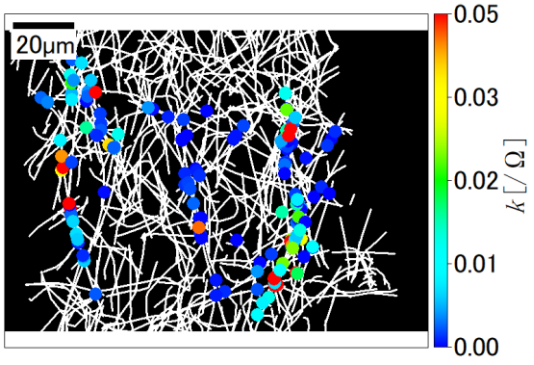

Figure 6. Contact electric conductivity distribution at the junction of which the sensitivity parameter S is greater than 1,000 K^2.

ACKNOWLEDGMENT

This work was supported by JSPS KAKENHI Grant Number 22K18769 and 21H01262.

REFERENCES

(1) Araki, T., Jiu, J., Nogi, M.,Koga, H., Nagao, S., Sugahara, T. and Suganuma, K. (2014): "Low haze transparent electrodes and highly conducting air dried films with ultra-long silver nanowires synthesized by one-step polyol method". *Nano Research*, Vol. 7, pp. 236-245.

(2) Lee, P., Lee, J., Lee, H., Yeo, J., Hong, S., Nam, K.H., Lee, D., Lee, S.S., Ko, S.H. (2012): "Highly stretchable and highly conductive metal electrode by very long metal nanowire percolation network". *Advanced Materials*, Vol. 24, pp. 3326-3332.

(3) Allen, T B., Hugh, G M., Claudia, G R., Mauro, S F. and John, J B. (2015): "Resistance of Single Ag Nanowire Junctions and Their Role in the Conductivity of Nanowire Networks". *ACS Nano*, Vol. 9, No. 11, pp. 11422-11429

(4) Sadeque, S., Gong, Y., Maize, K., Ziabri, A K., Mohammed, A M S., Shakouri, A. and Janes, D B. (2018): "Transient thermal response of hotspots in graphene–silver nanowire hybrid transparent conducting electrodes". *IEEE Transactions on Nanotechnology*, Vol. 17, No. 2, pp. 276-28.